NIH Public Access
Author Manuscript
Neuron. Author manuscript; available in PMC 2015 January 22.

Published in final edited form as:
Neuron. 2014 January 22; 81(2): 379–387. doi:10.1016/j.neuron.2013.11.004.

Distinct Ca^{2+} sources in dendritic spines of hippocampal CA1 neurons couple to SK and K_V4 channels

Kang Wang[1], **Mike T. Lin**[2], **John P. Adelman**[1,*], and **James Maylie**[3,*]

[1]Vollum Institute, Oregon Health & Science University, Portland, Oregon 97239, USA

[2]Department of Physiology, University of South Alabama 36688, USA

[3]Department of Obstetrics and Gynecology, Oregon Health & Science University, Portland, Oregon 97239, USA

SUMMARY

Ca^{2+}-activated SK channels and voltage-gated A-type K_V4 channels shape dendritic excitatory postsynaptic potentials (EPSPs) in hippocampal CA1 pyramidal neurons. Synaptically evoked Ca^{2+} influx through N-methyl-D-aspartate receptors (NMDARs) activates spine SK channels, reducing EPSPs and the associated spine head Ca^{2+} transient. However, results using glutamate uncaging implicated Ca^{2+} influx through SNX-482 (SNX) sensitive $Ca_V2.3$ (R-type) Ca^{2+} channels as the Ca^{2+} source for SK channel activation. The present findings show that using Schaffer collateral stimulation the effects of SNX and apamin are not mutually exclusive and SNX increases EPSPs independent of SK channel activity. Dialysis with 1,2-bis(o-aminophenoxy)ethane-N'N'N'-tetraacetic acid (BAPTA), application of 4-Aminopyridine (4-AP), expression of a $K_V4.2$ dominant negative subunit, and dialysis with a KChIPs antibody occluded the SNX-induced increase of EPSPs. The results suggest two distinct Ca^{2+} signaling pathways within dendritic spines, that links Ca^{2+} influx through NMDARs to SK channels and Ca^{2+} influx through R-type Ca^{2+} channels to $K_V4.2$-containing channels.

INTRODUCTION

Excitatory postsynaptic responses are initiated primarily by the activation of ionotropic glutamate receptors that depolarize the spine membrane potential and mediate Ca^{2+} influx. These effects provide for the secondary activation of voltage- and Ca^{2+}-dependent channels that can modulate and shape the synaptic responses. One example is Ca^{2+}-activated SK K^+ channels in CA1 pyramidal neurons that are activated locally by synaptically evoked Ca^{2+} influx. Their repolarizing influence reduces EPSPs and the associated spine head Ca^{2+} transient by promoting Mg^{2+} block of NMDARs. Therefore, blocking synaptic SK channels with apamin, a selective antagonist of SK channels, boosts EPSPs by as much as 50% and is reflected by an increase in the spine Ca^{2+} transient (Ngo-Anh et al., 2005). Immuno-electron microscopy demonstrated expression of one of the SK subunits, SK2, in the post-synaptic density (PSD) where SK2 immunoparticles were co-distributed with immunoparticles for

© 2013 Elsevier Inc. All rights reserved.

*Correspondences: mayliej@ohsu.edu (J.M.), adelman@ohsu.edu (J.P.A).

Publisher's Disclaimer: This is a PDF file of an unedited manuscript that has been accepted for publication. As a service to our customers we are providing this early version of the manuscript. The manuscript will undergo copyediting, typesetting, and review of the resulting proof before it is published in its final citable form. Please note that during the production process errors may be discovered which could affect the content, and all legal disclaimers that apply to the journal pertain.

Competing Interests Statement
The authors declare that they have no competing financial interests.

NIH-PA Author Manuscript
NIH-PA Author Manuscript
NIH-PA Author Manuscript

NIH-PA Author Manuscript

NIH-PA Author Manuscript

NIH-PA Author Manuscript

NMDARs (Lin et al., 2008). The colocalization of synaptic SK2-containing channels and NMDARs, taken together with the ability of either NMDAR blockers or dialysis with the Ca^{2+} buffer BAPTA, but not EGTA, in the patch pipette solution to occlude the effects of apamin suggested that SK channels and their Ca^{2+} source reside within 25–50 nm and that synaptically evoked Ca^{2+} influx through NMDARs activates SK2-containing channels (Ngo-Anh et al., 2005).

Subsequent work demonstrated that voltage-dependent $K_V4.2$-containing channels (Kim et al., 2007) and voltage-dependent Ca^{2+} channels in spines are also activated secondarily to ionotropic glutamate receptors. Among these channels are SNX-sensitive, R-type Ca^{2+} channels (Bloodgood and Sabatini, 2007). Using 2-photon laser photoactivation of caged glutamate onto single spines, uncaging-evoked synaptic responses (uEPSP) were measured at the soma. In addition, uncaging-evoked Ca^{2+} responses (Δ[Ca]uEPSP) were measured with Fluo-5F in the pipette using 2-photon laser scanning microscopy. Under these conditions, in the presence of SNX to block $Ca_V2.3$ Ca^{2+} channels, the standard uncaging-evoked stimulation, adjusted in voltage clamp to give a 10–15 pA response, yielded larger uEPSP and associated Δ[Ca]uEPSP compared to control cells. Importantly, in the presence of both apamin and SNX the uEPSP and Δ[Ca]uEPSP measurements were the same as those recorded in either SNX or apamin alone, indicating that SNX-mediated blockade of R-type channels occludes the SK-mediated inhibition of the uEPSP and the Δ[Ca]uEPSP (Bloodgood and Sabatini, 2007). Taken together, the results suggested that Ca^{2+} entry through SNX-sensitive R-type channels provides the Ca^{2+} for activating synaptic SK2-containing channels. In addition, the boosting effects of SNX on uncaging-evoked synaptic potentials and spine Ca^{2+} transients were absent in hippocampal pyramidal neurons from $Ca_V2.3$ null mice (Giessel and Sabatini, 2011). As previous results showed that synaptically evoked NMDAR activity is required to activate synaptic SK channels we therefore tested whether SNX occludes synaptically evoked activation of apamin sensitive SK channels in spines. We find that synaptic stimulations reveal the presence of two Ca^{2+} signaling pathways within the spine head, one that couples NMDARs with apamin-sensitive SK channels and another that couples SNX-sensitive R-type Ca^{2+} channels with 4-AP-sensitive $K_V4.2$ containing channels.

RESULTS

The effects of apamin and SNX are not mutually exclusive

Subthreshold EPSPs, evoked by stimulating the Schaffer collateral axons in stratum radiatum, were recorded in whole-cell current clamped CA1 neurons in acute slices from mouse hippocampus. To measure the effects of SK channels, EPSPs were recorded every 20 s before and after wash-in of apamin (100 nM). As previously reported (Ngo-Anh et al., 2005) and reproduced here, blocking SK channels with apamin increased the peak EPSP to 167 ± 12 % ($n = 13$, $P < 0.001$) of the control baseline, and pretreatment of the cells with D(-)-2-Amino-5-phosphonovaleric acid (D-AP5) (50 μM) to block NMDARs occluded the effect of apamin (101 ± 8%, $n = 6$).

To determine whether the effects of apamin and SNX were mutually exclusive for synaptically evoked responses, SNX (0.3 μM) was bath applied prior to apamin coapplication. Pretreating cells with SNX did not occlude the effect of subsequent apamin application that increased the peak EPSP to 152 ± 6% ($n = 15$, $P < 0.001$; Figure 1A) compared to baseline in SNX alone. Also, in the presence of apamin, SNX application increased the EPSP to 157 ± 8% compared to baseline in apamin alone ($n = 21$, $P < 0.001$; Figure 1C). The boosting of EPSPs by SNX does not require pre-block of SK channels by apamin; SNX in the absence of apamin increased the EPSP to 171.4 ± 10.9% compared to control ($n = 8$, $P < 0.001$), which was not different from that observed with apamin

NIH-PA Author Manuscript

NIH-PA Author Manuscript

NIH-PA Author Manuscript

pretreatment (P = 0.27). Similar results were obtained when $NiCl_2$ (100 μM) was used, which at low concentrations blocks R-type channels (Myoga and Regehr, 2011; Soong et al., 1993). In cells pretreated with Ni^{2+}, apamin application increased EPSPs to 150 ± 13% (n = 10; P < 0.05) while Ni^{2+} application to cells pretreated with apamin increased EPSPs to 137 ± 10% (n = 6; P < 0.05). Therefore, using synaptic stimulations, SNX or low concentrations of Ni^{2+}, and apamin independently increased EPSPs and their effects were not mutually exclusive.

Previously we showed that the apamin-induced enhancement of EPSPs was independent of the initial EPSP size from 1.1 to 7.9 mV (Lin et al., 2010b). To further examine whether apamin or SNX occlusion experiments were dependent on initial EPSP size, the enhancement of EPSPs by apamin or SNX were plotted against their initial EPSP amplitude (Figure 1B and 1D, respectively). The range of initial EPSP size for examining SNX occlusion of apamin in Figure 1A was from 0.8 to 3.8 mV. Fisher's r to z analysis of the EPSP increase by apamin in the presence of SNX compared to the initial EPSP size in SNX yielded no correlation. These results further demonstrate that SNX does not occlude the apamin response even for small initial EPSP sizes that are close to the average glutamate uncaging-evoked uEPSP of ~1 mV (Bloodgood and Sabatini, 2007). Additionally, the enhancement of EPSP amplitude by SNX in the presence of apamin was independent of initial EPSP size (Figure 1D).

Different from previous studies of postsynaptic R-type Ca^{2+} channels that used glutamate uncaging, responses to synaptic stimulation involve both presynaptic and postsynaptic components. In addition to postsynaptic localization, R-type channels may also be present in the presynaptic terminals (Parajuli et al., 2012) where they may influence glutamate release (Gasparini et al., 2001; Myoga and Regehr, 2011). To determine the effects of presynaptic R-type Ca^{2+} channels on glutamate release at Schaffer collateral to CA1 synapses, evoked excitatory postsynaptic currents (EPSCs) were measured in voltage clamp at −60 mV using the K-gluconate-based internal solution. As control, the effect of apamin was also determined. Under these conditions both SNX and apamin increased the peak EPSC by 37.4 ± 6.3% (n = 9, P < 0.001) and 33.2 ± 11.9% (n = 12, P < 0.05), respectively (Figure 2A and 2C). Total charge transfer was similarly increased (Figure 2B and 2D).

Given that postsynaptic conductances may not be controlled using a K^+-based internal solution due to voltage escape in the dendrites, voltage clamp recordings of EPSCs were measured using a Cs^+-based internal solution. D600 (200 μM), QX-314 (3.35 mM) and BAPTA (5 mM) were added to the pipette solution to block postsynaptic Ca^{2+}, Na^+ channels and Ca^{2+}-activated conductances, respectively, and D-AP5 was added to the bath solution to block NMDAR. Paired synaptic stimulations (50 ms interval) were delivered to monitor probability of release as measured by the peak and total charge transfer (area under the EPSC) of the EPSCs. Under these conditions, SNX (Figures 3A and 3B) reduced the amplitude to 79 ± 5% (n = 10, P < 0.05) but not the charge transfer of the first EPSC (88 ± 6%. n = 10; P = 0.12). The paired pulse ratios of EPSC peak and charge transfer were not significantly changed (117 ± 17% and 106 ± 10%, n = 10, respectively). In contrast, apamin had no effect on EPSC peak (93 ± 4%, n = 5) or charge transfer (Figure 3C and 3D). The paired pulse ratios of EPSC peak and charge transfer were also not affected by apamin (97 ± 6% and 98 ± 8%, n = 5, respectively).

These results confirm that glutamate release determined from EPSCs measured using the Cs^+-based internal solution with D600, QX-314 and BAPTA were not affected by apamin (Stackman et al., 2002) and that SNX, if anything, modestly decreases release (Gasparini et al., 2001). Therefore, the increase in EPSP by SNX is postsynaptic and is not occluded by apamin, and vice versa. Additionally, these results show that synaptic currents measured in

NIH-PA Author Manuscript

NIH-PA Author Manuscript

NIH-PA Author Manuscript

voltage clamp with a K^+-based internal solution in the absence of channel blockers may be influenced by changes in postsynaptic conductances.

One difference between the recording conditions used here for evoked EPSP measurements and the previous work that examined synaptic responses to uncaged glutamate is that in those previous experiments cells were filled with Fluo-5F (300 μM), a BAPTA-based fluorescent Ca^{2+} indicator as well as the Ca^{2+}-insensitive fluorescent dye, Alexa 594 (10 μM) (Bloodgood and Sabatini, 2007). Therefore, it is possible that the presence of 300 μM Fluo-5F, which would serve as a mobile Ca^{2+} buffer (K_d = 2.3 μM) could alter the dynamics of Ca^{2+} signaling within the spine head. To test this, cells were loaded with the standard pipette solution containing Fluo-5F (300 μM) and Alexa Fluor 594 (10 μM), and synaptically evoked EPSPs were examined for the effects of apamin and SNX. Under these conditions, apamin still increased peak EPSPs (133 ± 14% of control; n = 8, $P < 0.05$). Moreover, the effects of apamin were not occluded by SNX in the presence of the indicators; apamin still increased EPSP peaks compared to baseline recorded in SNX (140 ± 6%; n = 7, $P < 0.05$). These results show that the relatively low concentration of the BAPTA-based Ca^{2+} indicator, Fluo-5F did not markedly alter the independent boosting effects of apamin following SNX pretreatment.

The boosting effect of SNX requires Ca^{2+} influx

To determine whether Ca^{2+} influx through NMDARs is required for the boosting effect of SNX, baseline EPSPs were recorded in the presence of apamin and D-AP5 prior to application of SNX. Under these conditions SNX increased EPSPs to 142 ± 17% (n = 9; $P < 0.05$) (Figures 4A and 4B) suggesting that Ca^{2+} influx through NMDARs is not necessary for SNX boosting of EPSPs and that Ca^{2+} influx through SNX sensitive R-type Ca^{2+} channels is required for the boosting effect of SNX on synaptically evoked EPSPs. To test whether an increase in Ca^{2+} mobilization is required for SNX boosting of EPSPs, BAPTA (5 mM) was included in the internal patch pipette solution. Under these conditions, SNX still increased the EPSP to 142 ± 10% (n = 9, $P < 0.01$) in the presence of apamin. Increasing the concentration of BAPTA in the patch pipette solution to 10 mM blocked the increase in EPSP by SNX (EPSP peak: 110 ± 8% compared to baseline in apamin alone; n = 10) (Figures 4C and 4D). Therefore, an increase in Ca^{2+} mobilization is required for the boosting of EPSPs by SNX suggesting that Ca^{2+} entry through SNX sensitive R-type Ca^{2+} channels is necessary and that Ca^{2+} flowing into the spine head through R-type channels works within a very short intermolecular distance.

SNX boosting of synaptic responses requires $K_V4.2$-containing channels

These results raise the question of how blockade of an inward, depolarizing Ca^{2+} current increases EPSPs. In principle Ca^{2+} entry may activate a Ca^{2+}-dependent K^+ current that repolarizes the membrane potential, reducing EPSPs; blocking the Ca^{2+} source would boost EPSPs. However, the results presented above argue against that being an apamin sensitive SK channel. There are three other types of Ca^{2+}-dependent K^+ channels. Large conductance BK type K^+ channels, sensitive to Iberiotoxin (IbTx), are expressed in CA1 pyramidal neurons (Bloodgood and Sabatini, 2007), as are the as yet molecularly unidentified Ca^{2+}-dependent K^+ channels underlying the slow afterhyperpolarization (AHP) (Gerlach et al., 2004; Madison and Nicoll, 1984). The third class is IK1, a member of the SK family that is not apamin-sensitive but is blocked by the organic compound TRAM-34 (Wulff et al., 2000) and has a very limited expression profile in central neurons. To test whether any of these channel types are coupled to Ca^{2+} entry through SNX-sensitive R-type Ca^{2+} channels in CA1 pyramidal neurons, cells were pretreated with a cocktail of blockers (apamin, 100 nM; IbTx, 100 nM: carbachol, 5 μM: TRAM-34, 1 μM) to block SK, BK, sAHP and IK channels,

NIH-PA Author Manuscript

NIH-PA Author Manuscript

NIH-PA Author Manuscript

respectively. In the presence of this cocktail, SNX still increased EPSPs to 163 ± 15% of baseline (n = 6, P < 0.05) (Figures 5A and 5B).

How, then, does Ca^{2+} entry through SNX sensitive R-type Ca^{2+} channels boost EPSPs? The 4-AP sensitive A-type K^+ channels that contain $K_V4.2$ subunits are expressed in dendritic spines on CA1 pyramidal neurons and influence dendritic excitability and synaptic currents (Chen et al., 2006; Kim et al., 2007). Although these channels are intrinsically voltage-dependent, native $K_V4.2$-containing channels are multi-protein complexes that include the Ca^{2+} binding proteins, KChIPs, as auxiliary subunits (Rhodes et al., 2004). Recent reports have shown that in cerebellar stellate cells, Ca^{2+} entry through T-type Ca^{2+} channels acting via KChIPs shifts A-type channel availability to more negative potentials (Anderson et al., 2010). A similar shift in CA1 would increase the number of A-type channels available to open during an EPSP. Similarly, the activity-dependent trafficking of $K_V4.2$ in CA1 requires KChIPs (Lin et al., 2010a). To test whether SNX sensitive R-type Ca^{2+} channels boost EPSPs via effects on 4-AP sensitive A-type K^+ channels, baseline recordings were obtained in the presence of 4-AP (5 mM) and apamin prior to SNX application. In this case, SNX did not boost the EPSPs, being 90 ± 5% compared to baseline (n = 9; Figures 6A and 6B). These results suggest that the SNX boosting of EPSPs reveals an underlying coupling between R-type Ca^{2+} channels and activation of a 4-AP sensitive current such as the A-type K^+ channel. Alternatively, it is possible that SNX has off target effects at 0.3 μM and blocks 4-AP sensitive A-type channels. While this seems unlikely (Newcomb et al, 1998), we examined the effects of SNX (0.3 μM) on the 4-AP sensitive A-type transient outward current measured in voltage clamp in CA1 neurons. Although adequate voltage clamp control of CA1 neurons in slices is unlikely, the relative effects of SNX on the 4-AP sensitive current can be used to qualitatively test whether SNX blocks the A-type current. For these experiments, Ca^{2+}-free aCSF was supplemented with Mn^{2+} (2 mM) and TTX (1 μM) to block voltage-gated Ca^{2+} and Na^{2+} channels, respectively. Under these conditions, depolarization from −80 to 40 mV revealed an outward current that was partially blocked by 10 mM 4-AP (Figure 6C). Addition of SNX (0.3 μM) prior to addition of 4-AP had little effect on the total current and the 4-AP sensitive component was not blocked by SNX (Figure 6C, inset). The average effect of SNX on the 4-AP sensitive current was 96.8 ± 2.0% (n = 8, P = 0.15, Figure 6D). Furthermore, SNX had no effect on the non-inactivating, 4-AP insensitive component (102.1 ± 2.2%, P = 0.9). Thus, SNX does not block the A-type current in CA1 pyramidal neurons.

To determine whether the SNX boosting of EPSPs is mediated by an A-type channel that contains $K_V4.2$ subunits, a $K_V4.2$ dominant negative subunit, $K_V4.2$(W362F) (Kim et al., 2005) and eGFP were expressed in CA1 pyramidal neurons using *in-utero* electroporation of e16 embryos. Recordings were performed at 4–6 weeks of age. In eGFP positive cells, SNX application did not affect peak EPSPs, being 99 ± 7% compared to baseline in apamin (n = 9; Figures 7A and 7B). As a control, non-eGFP positive cells were studied and SNX increased the EPSP 159 ± 14% (n = 9, P < 0.01).

Finally, to test the hypothesis that KChIPs has an integral role in the SNX boosting of EPSPs, CA1 neurons were dialyzed with a pan-KChIPs antibody that has been shown to interrupt the coupling between T-type Ca^{2+} channels and A-type K^+ channels in cerebellar stellate cells (Anderson et al., 2010). Dialysis of CA1 pyramidal neurons with the pan-KChIPs antibody (20 μg/ml) occluded the boosting effect of SNX (105.7 ± 5.9%, n = 9, P = 0.37, Figure 8A, closed symbols, and 8B). As a control, SNX boosting of EPSPs in CA1 neurons dialyzed with a similar IgG2a isotype antibody (LRP4, 20 μg/ml) was 150.9 ± 13.6% (n = 6, P < 0.01, Figure 8A and 8C). Additionally, the pan-KChIPs antibody did not interfere with Ca^{2+} signaling for synaptic activation of SK channels as apamin boosting of

NIH-PA Author Manuscript

NIH-PA Author Manuscript

NIH-PA Author Manuscript

EPSPs was 143.4 ± 15.3% (n = 8, P < 0.05) in neurons dialyzed with the pan-KChIPs antibody.

DISCUSSION

The results presented here show that in CA1 pyramidal neurons blocking either apamin sensitive SK channels or SNX sensitive Ca^{2+} channels, presumably R-type, boosted synaptically evoked EPSPs, and the effects of apamin and SNX were not mutually exclusive. Pre-blocking NMDARs occluded the boosting of synaptic potentials by apamin, but not that of SNX, suggesting that Ca^{2+} entry through NMDARs is required for activation of synaptic SK channels but is not required for the effects of SNX. The boosting effect of SNX on the other hand required 4-AP sensitive $K_V4.2$-containing channels and KChIPs suggesting that Ca^{2+} influx through R-type Ca^{2+} channels is coupled to the availability of $K_V4.2$-containing channels.

The results are in contrast to those obtained by 2-photon laser uncaging of glutamate onto single spines in which the increase in uEPSPs was not different when SNX was present with or without apamin in the bath (Bloodgood and Sabatini, 2007). One advantage of glutamate uncaging is that presynaptic effects on transmitter release are bypassed. It has been previously reported at mossy fiber and associative–commissural synapses on CA3 pyramidal neurons that Ca^{2+} channels sensitive to low concentrations of Ni^{2+} contribute to glutamate release during minimal synaptic stimulation (Gasparini et al., 2001). Similarly, using a Cs^+ based internal solution optimized to minimize K^+, Na^+, Ca^{2+}, and Ca^{2+} activated channels, SNX but not apamin decreased the EPSC measured in voltage clamp. In contrast, if a K^+-based internal solution without pharmacological blockers of Na^+ and Ca^{2+}-channels is used, either apamin or SNX increased the EPSC measured in voltage clamp by 33% and 37%, respectively. Similarly, it has been shown that in cultured hippocampal neurons 4-AP increased mEPSCs using a K^+-based internal solution and the increase was greater at a holding potential of −60 mV compared to −80 mV (Kim et al., 2007). These results suggests that the consequence of voltage clamp escape is considerably greater when using a K^+-based internal solution to measure EPSCs, and that the EPSCs contain, in part, a postsynaptic outward current component. This may influence results obtained by glutamate uncaging when the uncaging laser power is adjusted to achieve a standard glutamate-evoked EPSC at −60 mV for different bath conditions using a K^+-based internal solution (Bloodgood and Sabatini, 2007). Consequently, a lower amount of glutamate uncaging may occur when SNX and/or apamin is in the bath compared to control solutions. It is therefore possible that the discrepancy between our results and those of Bloodgood and Sabatini, 2007 is the result of differences in glutamate uncaging due to adjusting the uncaging laser strength under different bath conditions where the neuron is not used as its own control. In contrast, for synaptically evoked glutamate release in which the neuron is used as its own control for measuring the effects of apamin or SNX revealed that SNX does not occlude the apamin mediated boosting of EPSPs.

Synaptic SK channel activity has also been shown to reduce EPSPs in cortical Layer 5 pyramidal neurons. In response to single synaptic stimulations, apamin boosted EPSPs and the apamin effect was occluded by blocking NMDAR, L-type Ca^{2+} channels, R-type Ca^{2+} channels, or Ca^{2+} release from intracellular stores leading to the conclusion that all of these Ca^{2+} sources contributed to activating synaptic SK channels and blocking any one of them was sufficient to occlude synaptic SK channel activation. Interestingly, in the presence of nicardipine to block L-type Ca^{2+} channels and SNX to block R-type Ca^{2+} channels, synaptic SK channels were activated by a train of stimuli, presumably due to increased Ca^{2+} influx through NMDARs, especially late in the train (Faber, 2010). Thus spine Ca^{2+} dynamics may differ across different classes of synapses.

NIH-PA Author Manuscript

NIH-PA Author Manuscript

NIH-PA Author Manuscript

One central result from CA1 spines is that either by glutamate uncaging or synaptic stimulations, blocking SNX-sensitive R-type Ca^{2+} channels boosts synaptic responses. The SNX effect did not require Ca^{2+} influx through NMDARs but did require a change in internal Ca^{2+}, as SNX did not increase synaptic responses when BAPTA was included in the internal pipette solution. Presumably the source of Ca^{2+} is influx through R-type channels. The finding that blocking an inward, depolarizing Ca^{2+} current increased rather than decreased EPSPs suggested that the effect may ultimately be mediated by suppression of a Ca^{2+}-activated K current. Yet, applying a cocktail of blockers to eliminate the canonical Ca^{2+}-activated K channels, (BK, SK, IK, and the sAHP channels) failed to occlude the SNX-induced increase in EPSPs. In contrast, application of 4-AP did occlude the SNX-induced increase of EPSPs, suggesting the involvement of an A-type voltage gated K^+ channel (I_A). $K_v4.2$ subunits are a major component of I_A in CA1 pyramidal neurons (Chen et al., 2006; Kim et al., 2005), and our results showing that expression of a $K_v4.2$ dominant negative abolishes the SNX boosting strongly support the model that SNX-sensitive Ca^{2+} channels are tightly coupled to regulation of availability of a $K_v4.2$-containing I_A channel.

$K_v4.2$ subunits are components of a multi-protein complex that includes the KChIPs (Rhodes et al., 2004), Ca^{2+} binding proteins that influence surface expression levels and biophysical attributes of K_v4-containing channels. Recently, it has been shown that K_v4-containing channels in cerebellar stellate cells form a molecular complex with T-type Ca^{2+} channels; Ca^{2+} influx through mifebridil sensitive T-type Ca^{2+} channels maintains the voltage dependence of availability of K_v4-containing channels in the physiological range, in a KChIPs dependent manner. Blocking T-type channels induced an ~10 mV hyperpolarizing shift in the voltage dependence of availability of I_A (Anderson et al., 2010). This shift was occluded by inclusion of 10 mM BAPTA or a pan-KChIPs antibody in the patch pipette internal solution, reflecting the close molecular proximity of K_v4-containing channels in complex with KChIPs and T-type channels. In CA1 pyramidal neurons, SNX-sensitive R-type Ca^{2+} channels are primarily expressed in dendritic spines (Bloodgood and Sabatini, 2007) and, while the precise mechanism is not yet established, the present results are consistent with a similar tight coupling to K_v4-containing channels such that Ca^{2+} influx through R-type Ca^{2+} channels shifts the voltage-dependence of availability of K_v4-containing channels allowing them to be activated during synaptic transmission. Consistent with this assertion is that dialysis with a pan-KChIPs antibody abolished the boosting of EPSPs by SNX.

SK2-containing channels and $K_v4.2$-containing channels are both expressed in dendritic spines on CA1 pyramidal neurons and their activities limit synaptic responses. Both channel types also undergo LTP-dependent endocytosis thereby contributing to the expression of LTP, and their trafficking is regulated by direct phosphorylation by PKA (Cai et al., 2004; Kim et al., 2007; Lin et al., 2008; Marino et al., 1998). The LTP- and PKA-dependent endocytosis of $K_v4.2$-containing channels, but not their contribution to basal synaptic responses, requires NMDAR activity. In this regard it is interesting that immuno-EM studies demonstrate that SK2 is expressed in the PSD and shows a similar synaptic distribution as seen for NMDARs, suggesting a close anatomical arrangement (Lin et al., 2008). In contrast, $K_v4.2$ immunoparticles were detected in postsynaptic spines but not directly in the PSD (Kim et al., 2007). Indeed, this extrasynaptic localization of $K_v4.2$ is similar to the predominantly extrasynaptic localization of $Ca_v2.3$ (Parajuli et al., 2012). Taken together with the ability of 10 mM BAPTA in the pipette solution to block the effect of SNX, these results suggest that $K_v4.2$-containing channels and SNX-sensitive R-type Ca^{2+} channels are closely coupled at extrasynaptic sites in spines. The co-localization of SK2-containing channels and NMDARs to the PSD and $K_v4.2$-containing channels and R-type Ca^{2+} channels to extrasynaptic sites therefore defines two Ca^{2+} signaling sources within spines. Interestingly, in the dendrites of CA1 pyramidal neurons, SK and K_v4-containing channels

NIH-PA Author Manuscript

NIH-PA Author Manuscript

NIH-PA Author Manuscript

serve complementary roles in shaping the time course and extent of branch specific dendritic excitability (Cai et al., 2004). Thus, SK channels and $K_V4.2$-containing channels may serve synergistic roles in regulating synaptic responses, the induction and expression of synaptic plasticity, and dendritic integration.

Many previous studies have concluded that fast excitatory transmission reflects glutamate receptor activation, as blocking AMPARs and NMDARs abolished the excitatory postsynaptic response. However, the present results demonstrate a large contribution from two types of K^+ channels. Indeed, apamin and SNX each boosted synaptic responses and the lack of occlusion demonstrates that their combined contribution approximately doubles the EPSP. Thus, together these two synaptic K^+ channels reduce the depolarizing component of EPSPs by at least 50%, suggesting that signaling cascades that alter their activities may potently regulate excitatory transmission. For example, cholinergic signaling in hippocampus by muscarinic ACh receptors, previously thought to boost EPSPs and facilitate the induction of LTP by increasing NMDAR activity (Aramakis et al., 1999; Marino et al., 1998; Markram and Segal, 1990) has recently been shown instead to decrease SK channel activity, leading to increased excitatory responses and LTP (Buchanan et al., 2010; Giessel and Sabatini, 2010). It is also important to note that in addition to the influence of repolarizing K^+ currents, Ca^{2+}-activated Cl^- channels (TMEM 16B) that are closely coupled to NMDARs similarly dampen EPSPs (Huang et al., 2012), adding to the inhibitory repertoire that modulates synaptic signals.

EXPERIMENTAL PROCEDURES

Slice preparation

All procedures were done in accordance with the guidelines of the Animal Care Committee of the Oregon Health & Science University. Hippocampal slices were prepared from C57BL/6J mice from post-natal week 4–6. Animals were anesthetized by isofluorane, and decapitated. The cerebral hemispheres were quickly removed and placed into cold artificial cerebrospinal fluid (aCSF) equilibrated with $95\%O_2/5\%CO_2$. Hippocampi were removed, placed onto an agar block, and transferred into a slicing chamber containing sucrose-aCSF. Transverse hippocampal slices (300 mm) were cut with a Leica VT1000s and transferred into a holding chamber containing regular aCSF (in mM: 125 NaCl, 2.5 KCl, 21.4 $NaHCO_3$, 1.25 NaH_2PO_4, 2.0 $CaCl_2$, 1.0 $MgCl_2$, 11.1 glucose) and equilibrated with $95\%O_2/5\%CO_2$. Slices were incubated at 35 °C for 30–45 min and then recovered at room temperature (22–24 °C) for ≥1 hr before recordings were performed.

In-utero electroporation

Timed-pregnant mice were anesthetized with isofluorane, their abdominal cavity cut open, and the uterine horns/sac exposed. Approximately 2 ml of DNA solution (~2 mg/ml) was injected into the lateral ventricle of e16 embryos, using a glass pipette pulled from thin walled capillary glass (TW150F-4, World Precision Instruments) and a Picospritzer III microinjection system (Parker Hannifin). The head of each embryo within its uterine sac was positioned between tweezer-type electrodes (CUY650P10; Sonidel Ltd.), and 5 square electric pulses (50V; 100 ms; 1 s intervals) were passed using an electroporator (CUY21; Sonidel Ltd.). After electroporation, the wall and skin of the abdominal cavity of the pregnant mouse was sutured-closed, and embryos were allowed to develop normally.

Electrophysiology

Slices were perfused with aCSF equilibrated with $95\%O_2/5\%CO_2$ at a flow rate of 1 ml/min. All experiments were performed at room temperature (22–24 °C). CA1 pyramidal cells were visualized with infrared–differential interference contrast optics (Zeiss Axioskop 2FS) and a

NIH-PA Author Manuscript

NIH-PA Author Manuscript

NIH-PA Author Manuscript

CCD camera (Sony). Whole-cell patch-clamp recordings were obtained from CA1 pyramidal cells using an Axopatch 1D (Axon Instruments) interfaced to an ITC-16 analog-to-digital converter (Heka Instruments, Bellmore, NY) and transferred to a computer using Patchmaster software (Heka Instruments, Bellmore, NY). Patch pipettes (open pipette resistance, 2.5–3.5 MΩ), for EPSP were filled with either a K-gluconate internal solution containing (in mM) 133 K-gluconate, 4 KCl, 4 NaCl, 1 $MgCl_2$, 10 HEPES, 4 MgATP, 0.3 Na_3GTP, 10 K_2-phosphocreatine (pH 7.3) or a $KMeSO_4$ internal solution containing (in mM) 140 $KMeSO_4$, 8 NaCl, 1 $MgCl_2$, 10 HEPES, 5 MgATP, 0.4 Na_3GTP, 0.05 EGTA (pH 7.3). EPSPs were recorded in whole-cell current-clamp mode. Input and access resistances were monitored with a 25 pA hyperpolarizing step applied at the end of each trace. All current clamp recordings used cells with a stable input resistance (range: 130–300 MΩ) and access resistance (range: 15–25 MΩ) that did not change by more than 20%. All recordings were from cells with a resting membrane potential between −70 and −60 mV. A bias current was applied to maintain the membrane potential at −65 mV. Series resistance was not electronic compensated. For EPSC recordings in voltage clamp mode, patch pipettes were filled with a Cs^+ based solution containing (in mM) 130 $CsMeSO_4$, 10 CsCl, 10 HEPES, 0.4 Na_3GTP, 2 MgATP, 10 Tris-Phosphocreatine, 3.35 QX-314, 0.2 D600, 5 BAPTA (pH with CsOH to 7.2). Series resistance was not electronic compensated. Input resistance was monitored with a 5 mV hyperpolarizing step applied at the beginning of each trace. All voltage clamp recordings used cells with a stable input and access resistances that did not change by more than 20%. For whole cell recording of A-type outward K^+ currents, patch pipettes were filed with (120 K-gluconate, 20 KCl, 10 HEPES, 0.2 EGTA, 8 NaCl, 4 MgATP, 0.3 Na_3GTP and 14 Tris-phosphocreatine, pH 7.3). For whole cell recording of A-type currents, the series resistance was ~80% compensated. Input resistance was monitored with a 5 mV hyperpolarizing step applied at the beginning of each trace. All voltage clamp recordings used cells with a stable input and access resistances that did not change by more than 20%.

Synaptic stimulation

Presynaptic axons in stratum radiatum were stimulated using capillary glass pipettes filled with aCSF, with a tip diameter of ~5 μm, connected to an Iso-Flex stimulus isolation unit (A.M.P.I., Israel). Stimulation electrodes were placed at ~100 μm from the soma and ~20 μm adjacent to the dendrite of the recorded cell. GABAergic blockers SR95531 (2 μM) and CGP55845 (1 μM) were present to reduce $GABA_A$ and $GABA_B$ contributions, respectively. To prevent epileptic discharges in the presence of GABAergic blockers, the CA3 region was microdissected out before recording. The input resistance was determined from a 25-pA hyperpolarizing current injection pulse given 500 ms after each synaptically evoked EPSP. Subthreshold EPSPs were elicited by 100-μs current injections that were approximately one-third of the stimulus required for evoking an action potential. All recordings used cells with a resting membrane potential less than −60mV that did not change by more than 2 mV during an experiment and with a stable input resistance that did not change by more than 20%.

Data analysis

Data were analyzed using IGOR (WaveMetrics, Lake Oswego, OR). Data are expressed as mean ± s.e.m. Paired t-tests or Wilcoxon-Mann-Whitney 2-sample rank test was used to determine significance; $P < 0.05$ was considered significant.

Pharmacology

Apamin was from Calbiochem, D-AP5, QX314, SR95531, and CGP55845 were from Tocris Cookson, SNX-482 was from Peptides International, Iberiotoxin and TRAM-34 were from Alomone, carbachol and 4-AP were from Sigma. Pan-KChIPs (K55/82) and LRP4

NIH-PA Author Manuscript

NIH-PA Author Manuscript

NIH-PA Author Manuscript

(N207/27) antibodies were obtained from UC Davis/NIH NeuroMab Facility (Antibodies Incorporated, Davis, Ca).

Acknowledgments

We thank Dr. Bernardo Sabatini for helpful discussions. We also thank Dr. Dax Hoffman for the $K_V4.2$ dominant negative construct. This work was supported by National Institutes of Health grants to J.M. and J.P.A.

Literature Cited

Anderson D, Mehaffey WH, Iftinca M, Rehak R, Engbers JD, Hameed S, Zamponi GW, Turner RW. Regulation of neuronal activity by Cav3-Kv4 channel signaling complexes. Nat Neurosci. 2010; 13:333–337. [PubMed: 20154682]

Aramakis VB, Bandrowski AE, Ashe JH. Role of muscarinic receptors, G-proteins, and intracellular messengers in muscarinic modulation of NMDA receptor-mediated synaptic transmission. Synapse. 1999; 32:262–275. [PubMed: 10332802]

Bloodgood BL, Sabatini BL. Nonlinear regulation of unitary synaptic signals by CaV(2.3) voltage-sensitive calcium channels located in dendritic spines. Neuron. 2007; 53:249–260. [PubMed: 17224406]

Buchanan KA, Petrovic MM, Chamberlain SE, Marrion NV, Mellor JR. Facilitation of long-term potentiation by muscarinic M(1) receptors is mediated by inhibition of SK channels. Neuron. 2010; 68:948–963. [PubMed: 21145007]

Cai X, Liang CW, Muralidharan S, Kao JP, Tang CM, Thompson SM. Unique roles of SK and Kv4.2 potassium channels in dendritic integration. Neuron. 2004; 44:351–364. [PubMed: 15473972]

Chen X, Yuan LL, Zhao C, Birnbaum SG, Frick A, Jung WE, Schwarz TL, Sweatt JD, Johnston D. Deletion of Kv4.2 gene eliminates dendritic A-type K^+ current and enhances induction of long-term potentiation in hippocampal CA1 pyramidal neurons. J Neurosci. 2006; 26:12143–12151. [PubMed: 17122039]

Faber ES. Functional interplay between NMDA receptors, SK channels and voltage-gated Ca^{2+} channels regulates synaptic excitability in the medial prefrontal cortex. J Physiol. 2010; 588:1281–1292. [PubMed: 20194128]

Gasparini S, Kasyanov AM, Pietrobon D, Voronin LL, Cherubini E. Presynaptic R-type calcium channels contribute to fast excitatory synaptic transmission in the rat hippocampus. J Neurosci. 2001; 21:8715–8721. [PubMed: 11698583]

Gerlach AC, Maylie J, Adelman JP. Activation kinetics of the slow afterhyperpolarization in hippocampal CA1 neurons. Pflugers Arch. 2004; 448:187–196. [PubMed: 14727118]

Giessel AJ, Sabatini BL. M1 muscarinic receptors boost synaptic potentials and calcium influx in dendritic spines by inhibiting postsynaptic SK channels. Neuron. 2010; 68:936–947. [PubMed: 21145006]

Giessel AJ, Sabatini BL. Boosting of synaptic potentials and spine Ca transients by the peptide toxin SNX-482 requires alpha-1E-encoded voltage-gated Ca channels. PLoS One. 2011; 6:e20939. [PubMed: 21695265]

Huang WC, Xiao S, Huang F, Harfe BD, Jan YN, Jan LY. Calcium-activated chloride channels (CaCCs) regulate action potential and synaptic response in hippocampal neurons. Neuron. 2012; 74:179–192. [PubMed: 22500639]

Kim J, Jung SC, Clemens AM, Petralia RS, Hoffman DA. Regulation of dendritic excitability by activity-dependent trafficking of the A-type K^+ channel subunit Kv4.2 in hippocampal neurons. Neuron. 2007; 54:933–947. [PubMed: 17582333]

Kim J, Wei DS, Hoffman DA. Kv4 potassium channel subunits control action potential repolarization and frequency-dependent broadening in rat hippocampal CA1 pyramidal neurones. J Physiol. 2005; 569:41–57. [PubMed: 16141270]

Lin L, Sun W, Wikenheiser AM, Kung F, Hoffman DA. KChIP4a regulates Kv4.2 channel trafficking through PKA phosphorylation. Mol Cell Neurosci. 2010a; 43:315–325. [PubMed: 20045463]

NIH-PA Author Manuscript

NIH-PA Author Manuscript

NIH-PA Author Manuscript

Lin MT, Lujan R, Watanabe M, Adelman JP, Maylie J. SK2 channel plasticity contributes to LTP at Schaffer collateral-CA1 synapses. Nat Neurosci. 2008; 11:170–177. [PubMed: 18204442]

Lin MT, Lujan R, Watanabe M, Frerking M, Maylie J, Adelman JP. Coupled activity-dependent trafficking of synaptic SK2 channels and AMPA receptors. The Journal of neuroscience : the official journal of the Society for Neuroscience. 2010b; 30:11726–11734. [PubMed: 20810893]

Madison DV, Nicoll RA. Control of the repetitive discharge of rat CA1 pyramidal neurons *in vitro*. J Physiol. 1984; 354:319–331. [PubMed: 6434729]

Marino MJ, Rouse ST, Levey AI, Potter LT, Conn PJ. Activation of the genetically defined m1 muscarinic receptor potentiates N-methyl-D-aspartate (NMDA) receptor currents in hippocampal pyramidal cells. Proc Natl Acad Sci U S A. 1998; 95:11465–11470. [PubMed: 9736760]

Markram H, Segal M. Acetylcholine potentiates responses to N-methyl-D-aspartate in the rat hippocampus. Neurosci Lett. 1990; 113:62–65. [PubMed: 1973273]

Myoga MH, Regehr WG. Calcium microdomains near R-type calcium channels control the induction of presynaptic long-term potentiation at parallel fiber to purkinje cell synapses. J Neurosci. 2011; 31:5235–5243. [PubMed: 21471358]

Ngo-Anh TJ, Bloodgood BL, Lin M, Sabatini BL, Maylie J, Adelman JP. SK channels and NMDA receptors form a Ca^{2+}-mediated feedback loop in dendritic spines. Nat Neurosci. 2005; 8:642–649. [PubMed: 15852011]

Parajuli LK, Nakajima C, Kulik A, Matsui K, Schneider T, Shigemoto R, Fukazawa Y. Quantitative Regional and Ultrastructural Localization of the Cav2.3 Subunit of R-type Calcium Channel in Mouse Brain. J Neurosci. 2012; 32:13555–13567. [PubMed: 23015445]

Rhodes KJ, Carroll KI, Sung MA, Doliveira LC, Monaghan MM, Burke SL, Strassle BW, Buchwalder L, Menegola M, Cao J, et al. KChIPs and Kv4 alpha subunits as integral components of A-type potassium channels in mammalian brain. J Neurosci. 2004; 24:7903–7915. [PubMed: 15356203]

Soong TW, Stea A, Hodson CD, Dubel SJ, Vincent SR, Snutch TP. Structure and functional expression of a member of the low voltage-activated calcium channel family. Science. 1993; 260:1133–1136. [PubMed: 8388125]

Stackman RW, Hammond RS, Linardato s E, Gerlach A, Maylie J, Adelman JP, Tzounopoulos T. Small conductance Ca^{2+}-activated K^+ channels modulate synaptic plasticity and memory encoding. The Journal of neuroscience : the official journal of the Society for Neuroscience. 2002; 22:10163–10171. [PubMed: 12451117]

Wulff H, Miller MJ, Hansel W, Grissmer S, Cahalan MD, Chandy KG. Design of a potent and selective inhibitor of the intermediate-conductance Ca^{2+}-activated K^+ channel, IKCa1: a potential immunosuppressant. Proc Natl Acad Sci U S A. 2000; 97:8151–8156. [PubMed: 10884437]

NIH-PA Author Manuscript

NIH-PA Author Manuscript

NIH-PA Author Manuscript

HIGHLIGHTS

- Blocking R-type Ca^{2+} channels with SNX or Ni^{2+} increases synaptically evoked EPSPs
- Synaptic activation of SK channels is not coupled to R-type Ca^{2+} channel activation
- Kv4 channel activation is coupled to synaptic activation of R-type Ca^{2+} channels
- Distinct Ca^{2+} sources in hippocampal spines couple to SK and Kv4 channels

NIH-PA Author Manuscript
NIH-PA Author Manuscript
NIH-PA Author Manuscript

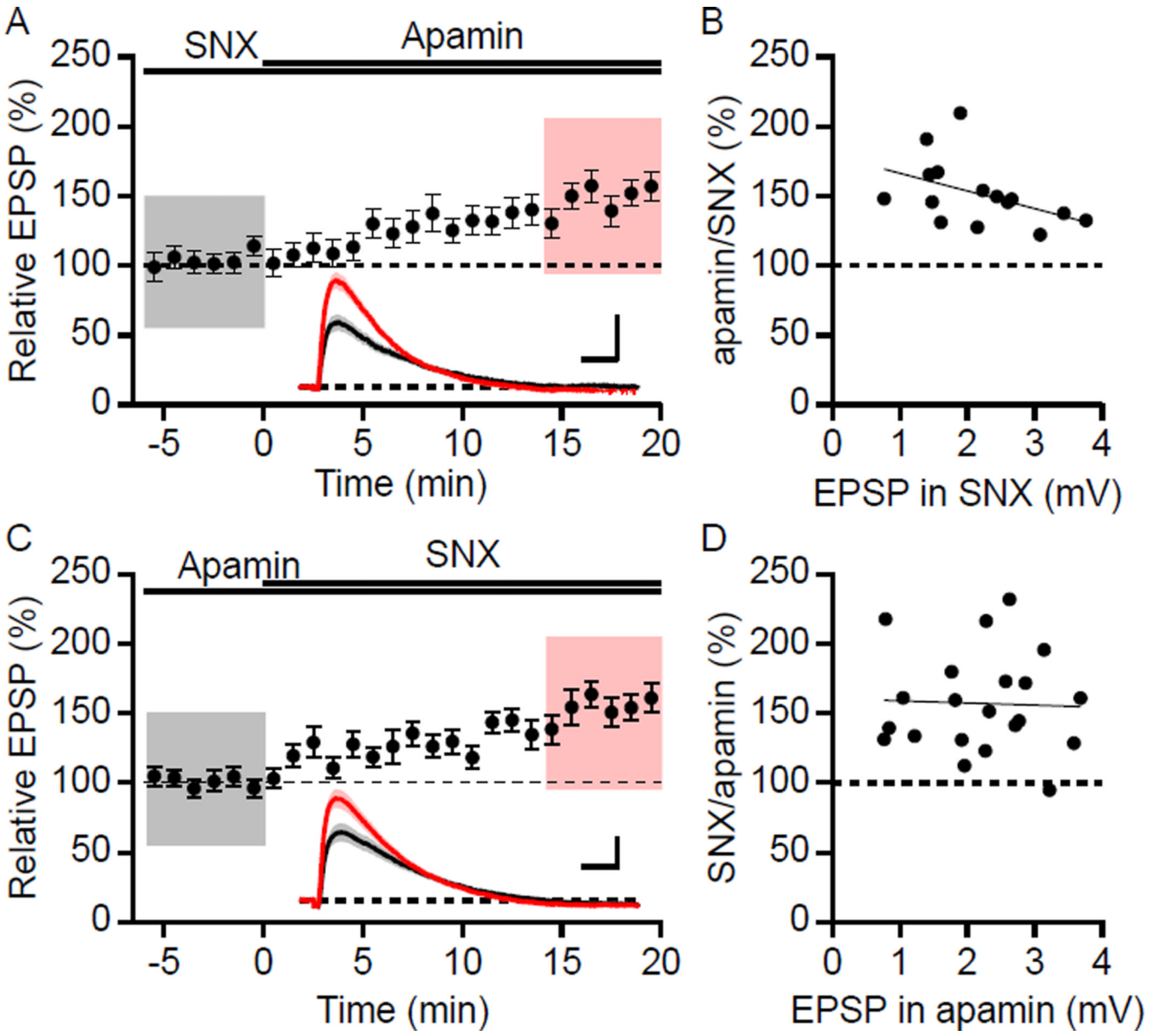

Figure 1. Boosting of EPSPs by SNX and apamin is not mutually exclusive

(A) Time course of the normalized EPSP amplitude (mean ± s.e.m.) for baseline in SNX and during wash-in of apamin as indicated above (n = 15). Inset shows the average of 18 EPSPs taken from indicated shaded time points in SNX (black; 6 min baseline) and 14–20 min after co-application of apamin (red); shaded areas are mean ± s.e.m. Scale bars: 1 mV and 25 ms. (B) Plot of relative boosting of EPSPs by apamin in the presence of SNX versus the initial EPSP in SNX. The line represents a least-square fit of the data to a liner function. (C) Similar to panel A, except baseline in apamin and during wash-in of SNX (n = 21). Insets: Averaged EPSPs (± s.e.m., shaded areas) in apamin (black) and after co-application of SNX (red). Scale bars: 1 mV and 25 ms. (D) Plot of relative boosting of EPSPs by SNX in the presence of apamin versus the initial EPSP in apamin. The line represents a least-square fit of the data to a liner function.

NIH-PA Author Manuscript
NIH-PA Author Manuscript
NIH-PA Author Manuscript

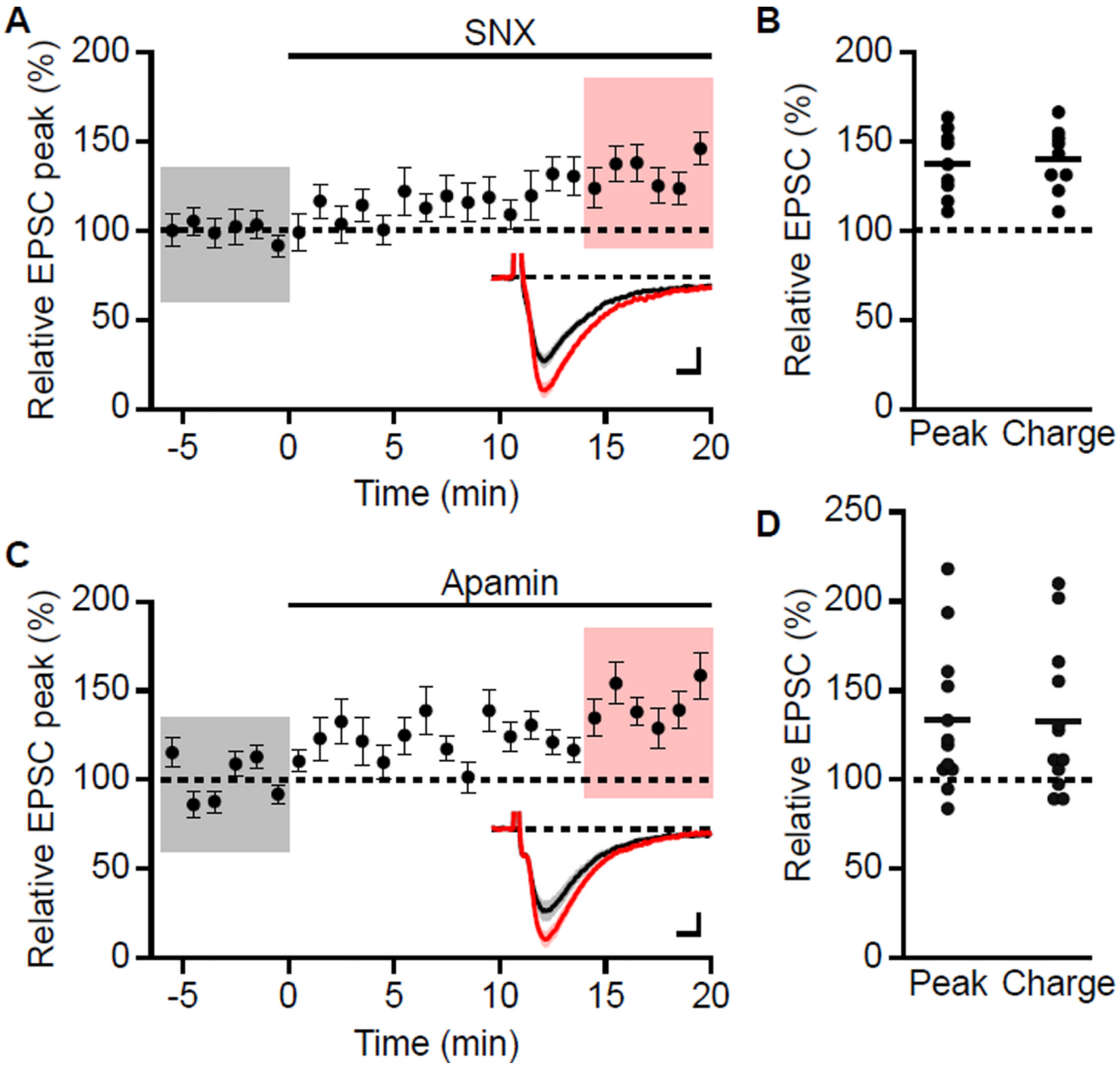

Figure 2. SNX and apamin increases EPSC measured with a K^+ -based internal solution

(A) Time course of relative increase in peak EPSC by 0.3 μM SNX (mean ± s.e.m., n = 9). Insets: averaged of 18 EPSCs ± s.e.m. (shaded areas) for taken from indicated shaded time points for baseline (black) and 14–20 min after wash-in of SNX (red). Scale bars: 10 pA and 5 ms. (B) Scatter plot of relative EPSC peak and charge in SNX compared to baseline from the individual slices in panel A. Horizontal bar reflects mean response. (C) Time course of relative increase in peak EPSC by 100 nM apamin (mean ± s.e.m., n = 12). Insets: averaged of 18 EPSCs ± s.e.m. (shaded areas) taken from indicated shaded time points for baseline (black) and 14–20 min after wash-in of apamin (red). Scale bars: 10 pA and 5 ms. (D) Scatter plot of relative EPSC peak and charge in apamin compared to baseline from the individual slices in panel C. Horizontal bar reflects mean response.

NIH-PA Author Manuscript
NIH-PA Author Manuscript
NIH-PA Author Manuscript

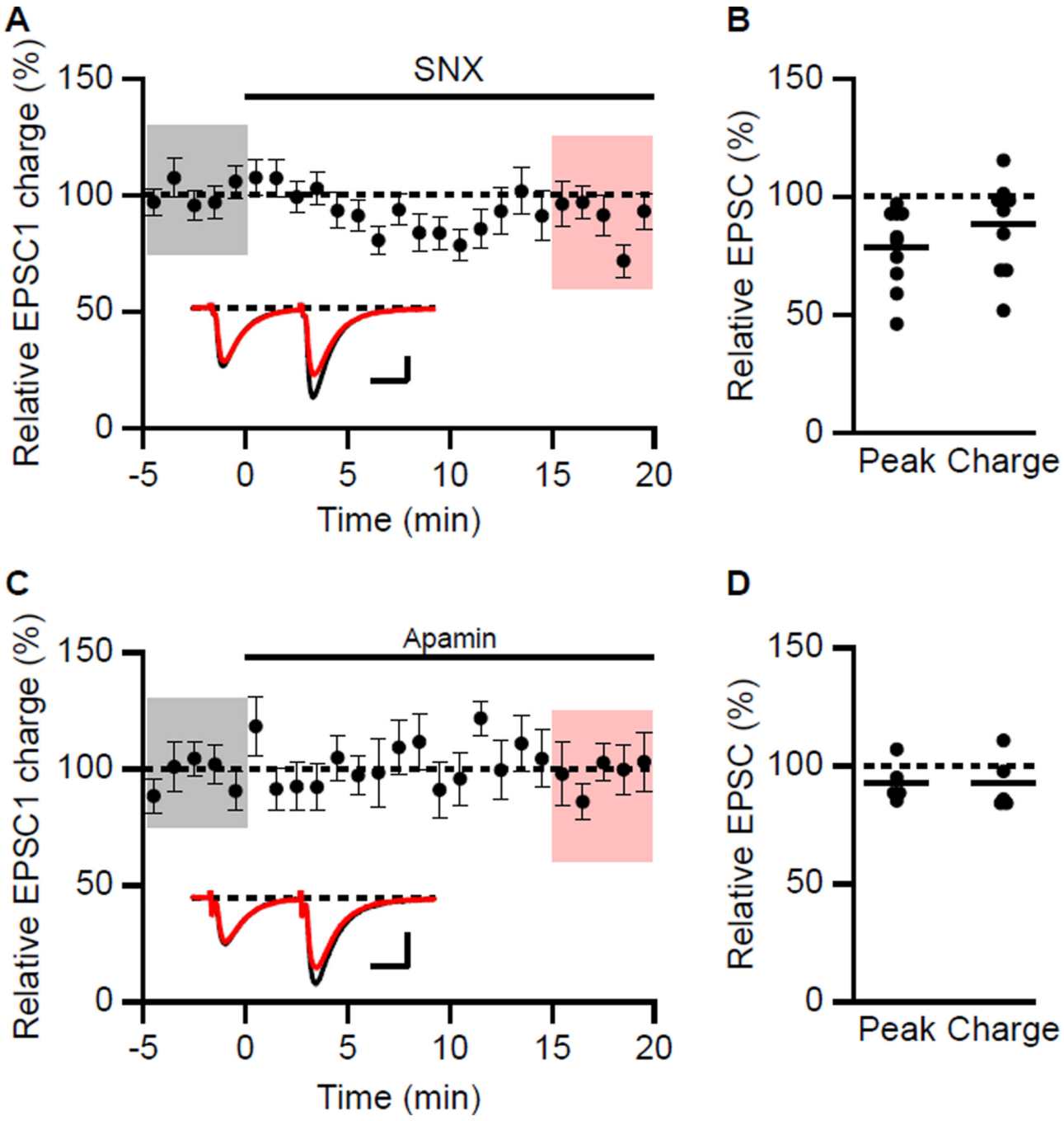

Figure 3. Effect of SNX on synaptic transmission in voltage clamp

(A) Time course of the normalized charge transfer of the first EPSC (EPSC1) (mean ± s.e.m.) for baseline and during wash-in of SNX (n = 10). Insets: averaged of 15 paired EPSCs ± s.e.m. (shaded areas) taken from indicated shaded time points for baseline (black) and 15–20 min after wash-in of SNX (red). Scale bars: 50 pA and 20 ms. (B) Scatter plot of relative EPSC1 peak and charge in SNX compared to baseline from the individual slices in panel A. Horizontal bar reflects mean response. (C) Time course of the normalized charge transfer of the first EPSC (EPSC1) (mean ± s.e.m.) for baseline and during wash-in of apamin (n = 5). Insets: averaged of 15 paired EPSCs ± s.e.m. (shaded areas) taken from indicated shaded time points for baseline (black) and 15–20 min after wash-in of apamin

(red). Scale bars: 50 pA and 20 ms. (D) Scatter plot of relative EPSC1 peak and charge in apamin compared to baseline from the individual slices in panel A. Horizontal bar reflects mean response.

NIH-PA Author Manuscript
NIH-PA Author Manuscript
NIH-PA Author Manuscript

NIH-PA Author Manuscript
NIH-PA Author Manuscript
NIH-PA Author Manuscript

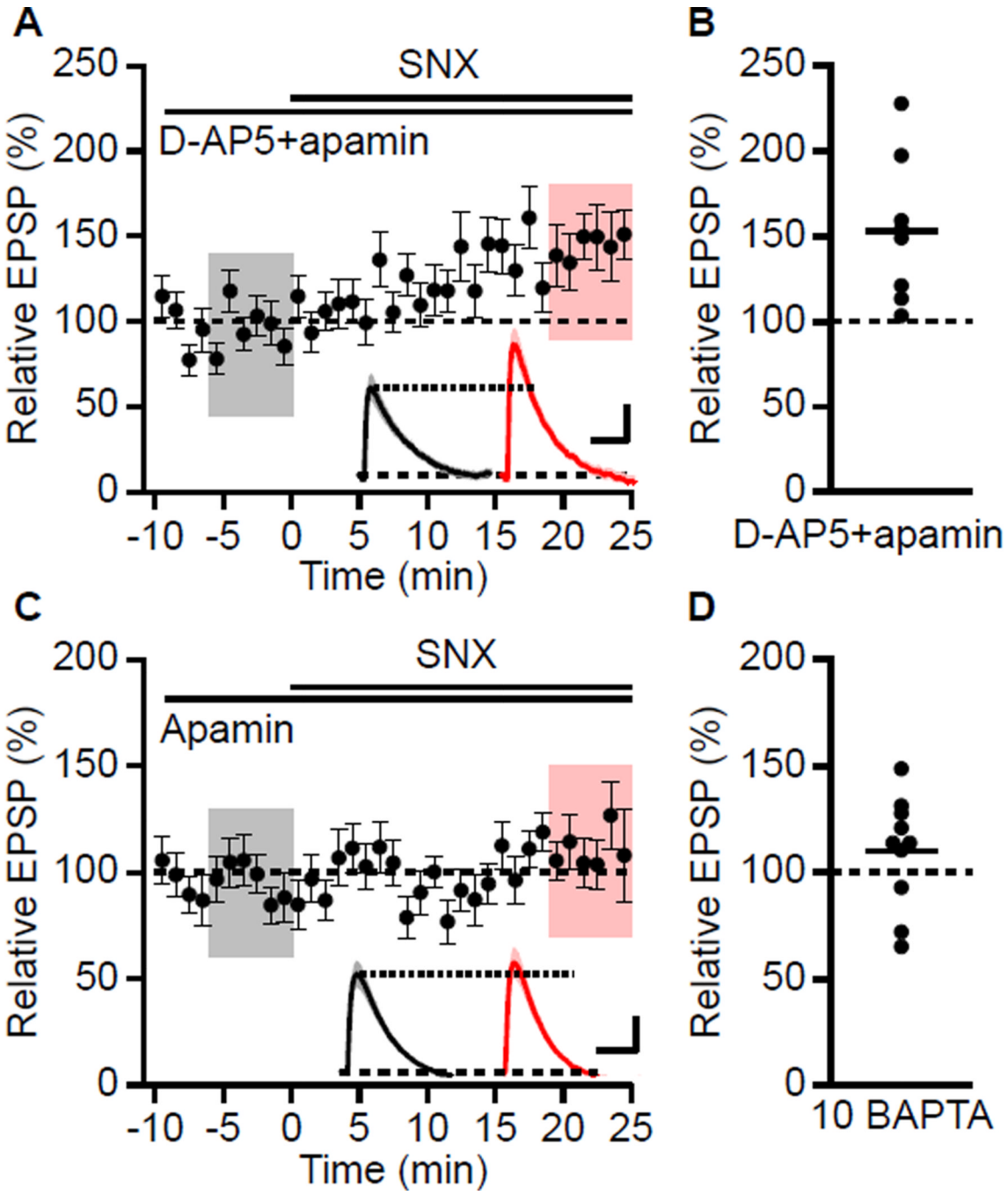

Figure 4. Boosting of EPSPs by SNX is NMDAR-independent and Ca^{2+}-dependent

(A) Time course of the normalized EPSP amplitude (mean ± s.e.m., n = 9) for baseline in dAP5 and apamin, and during wash-in of SNX as indicated above. Inset: Average of 18 EPSPs taken from indicated shaded time points in dAP5 and apamin (baseline; black) and 19–25 min after SNX wash-in (red); shaded areas are ± s.e.m. Scale bars: 1 mV and 50 ms. (B) Scatter plot of relative EPSP peak in SNX compared to baseline in D-AP5 and apamin from the individual slices in panel A. Horizontal bar reflects mean response. (C) Time course of the normalized EPSP amplitude (mean ± s.e.m., n = 10) recorded with BAPTA in the internal solution, for baseline in apamin and during wash-in of SNX as indicated above. Inset: Average of 18 EPSPs taken from indicated shaded time points in apamin (baseline;

black) and 19–25 min after SNX wash-in (red); shaded areas are ± s.e.m. Scale bars: 0.5 mV and 50 ms. (D) Scatter plot of relative EPSP peak in SNX compared to baseline in apamin from the individual slices in panel C. Horizontal bar reflects mean response.

NIH-PA Author Manuscript
NIH-PA Author Manuscript
NIH-PA Author Manuscript

NIH-PA Author Manuscript

NIH-PA Author Manuscript

NIH-PA Author Manuscript

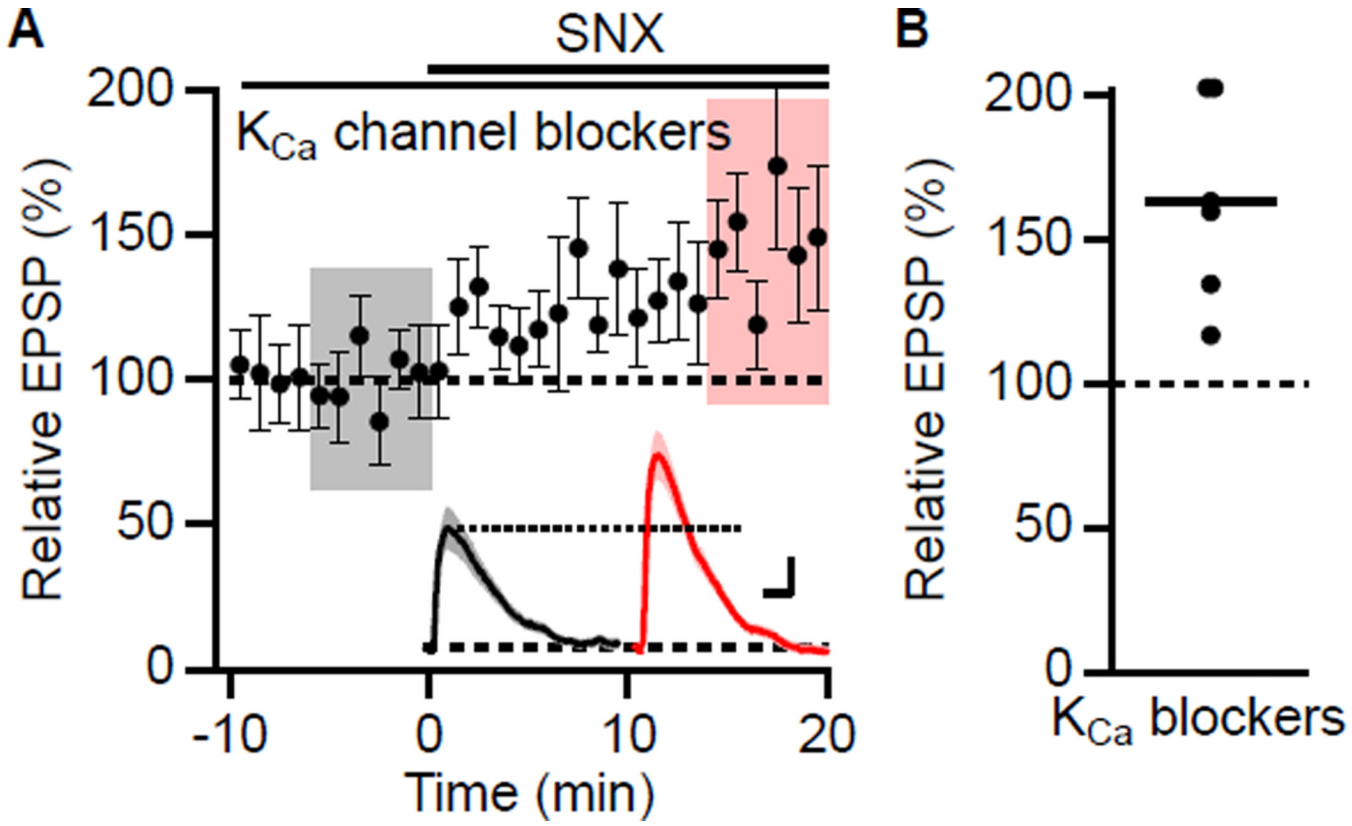

Figure 5. Canonical K_{Ca} channels do not mediate the boosting effect of SNX

(A) Time course of the normalized EPSP amplitude (mean ± s.e.m., n = 6) for baseline in a cocktail of apamin, IbTx, Tram34, and carbachol, and during wash-in of SNX as indicated above. Inset shows average of 18 EPSPs taken from indicated shaded time points in the cocktail of K_{Ca} blockers (baseline; black) and 14–20 min after SNX wash-in (red); shaded areas are ± s.e.m. Scale bars: 0.5 mV and 25 ms. (B) Scatter plot of relative EPSP peak in SNX compared to baseline in the cocktail of K_{Ca} channel antagonists from the individual slices in panel A. Horizontal bar reflects mean response.

NIH-PA Author Manuscript
NIH-PA Author Manuscript
NIH-PA Author Manuscript

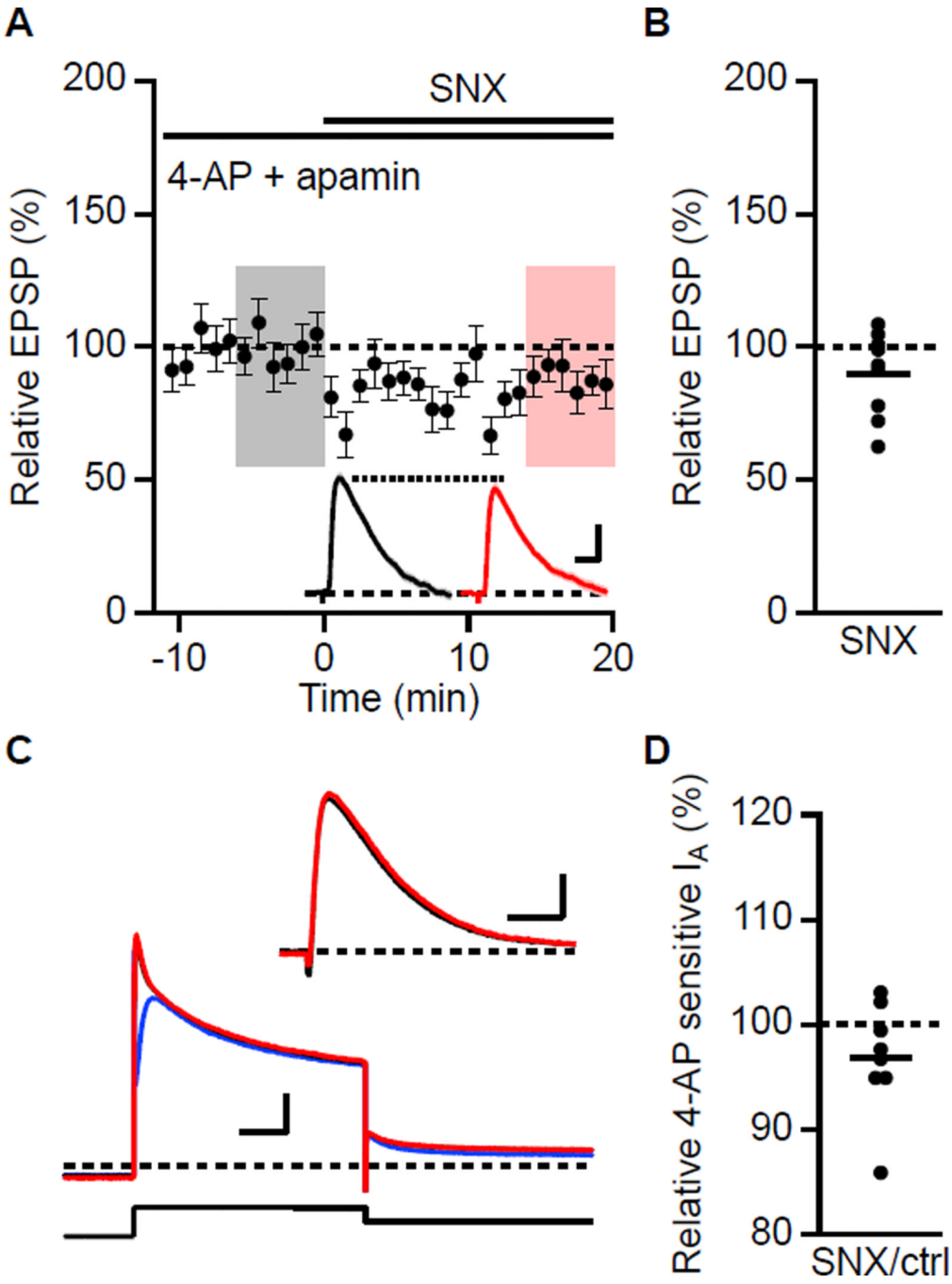

Figure 6. 4-AP occludes the boosting effect of SNX

(A) Time course of the normalized EPSP amplitude (mean ± s.e.m., n = 9) for baseline in 4-AP and apamin, and during wash-in of SNX as indicated above. Inset shows average of 18 EPSPs taken from indicated shaded time points in 4-AP and apamin (baseline; black) and 14–20 min after SNX wash-in (red); shaded areas are ± s.e.m. Scale bars: 1.0 mV and 25 ms. (B) Scatter plot of relative EPSP peak in SNX compared to baseline in 4-AP from the individual slices in panel A. Horizontal bar reflects mean response. (C) SNX does not block 4-AP sensitive A-type current (I_A) measured in voltage clamp. Slices were bathed in nominally Ca^{2+}-free aCSF containing TTX (1 μM) and Mn^{2+} (2 mM). In whole cell voltage clamp, A-type outward currents were elicited with 1 s depolarization to 40 mV from a

NIH-PA Author Manuscript

NIH-PA Author Manuscript

NIH-PA Author Manuscript

holding potential of −80 mV followed by repolarization to −20 mV. Representative traces of outward current in control (black), subsequent addition of SNX (red) and SNX plus 4-AP (blue). Inset: 4-AP sensitive current in control (black) and SNX (red). Scale bars: 1 nA and 20 ms. (D) Scatter plot of individual slices for relative 4-AP sensitive I_A current in SNX. Horizontal bar reflects mean response.

NIH-PA Author Manuscript
NIH-PA Author Manuscript
NIH-PA Author Manuscript

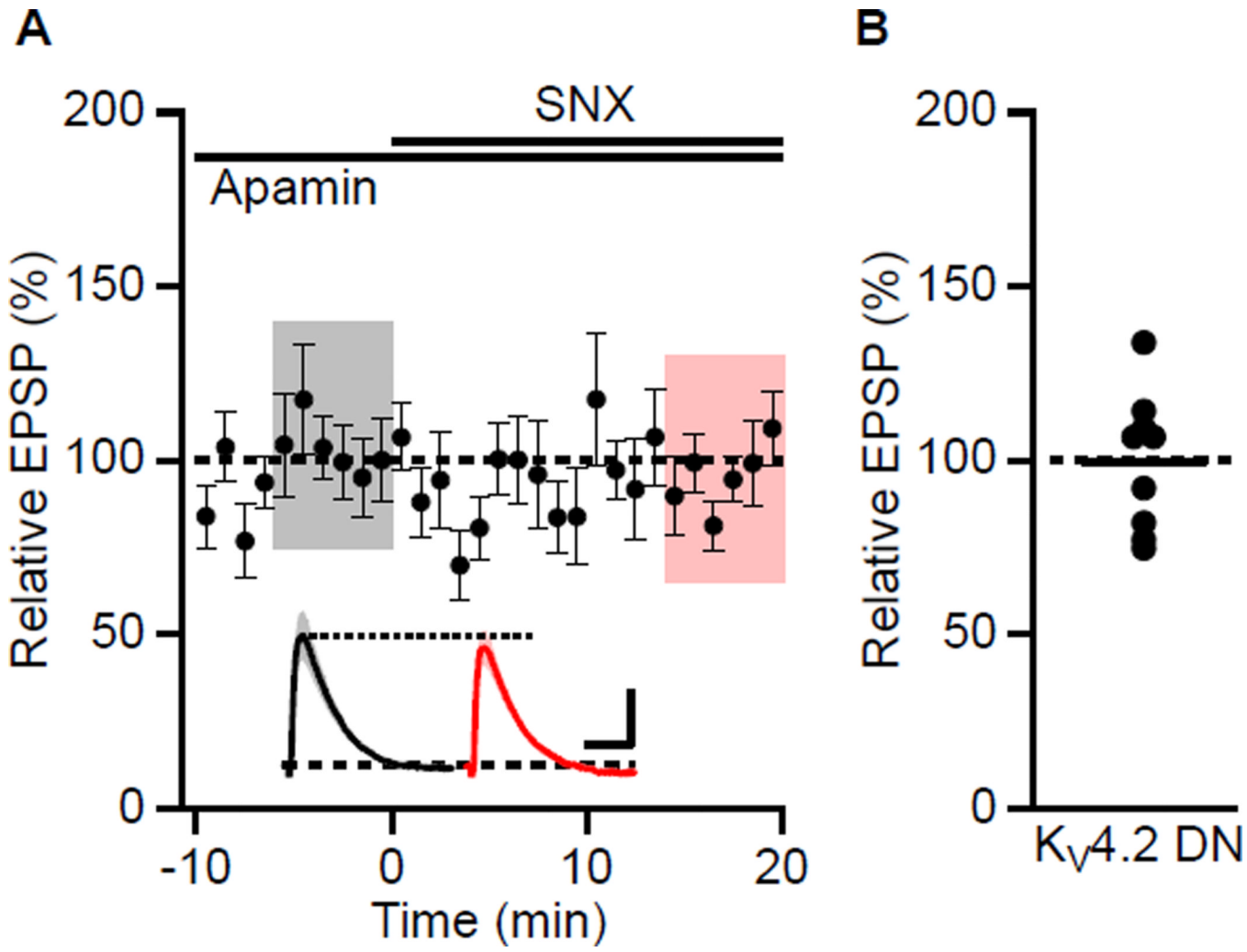

Figure 7. Expression of K_V4.2(W362F) abolishes the boosting effect of SNX

(A) Recordings from cells expressing K_V4.2(W362F). Time course of the normalized EPSP amplitude (mean ± s.e.m., n = 9) for baseline in apamin, and during wash-in of SNX as indicated above. Inset shows average of 18 EPSPs taken from indicated shaded time points in apamin (baseline; black) and 14–20 min after SNX wash-in (red); shaded areas are ± s.e.m. Scale bars: 1 mV and 50 ms. (B) Scatter plot of relative EPSP peak in SNX compared to baseline in apamin from the individual slices in panel A. Horizontal bar reflects mean response.

NIH-PA Author Manuscript
NIH-PA Author Manuscript
NIH-PA Author Manuscript

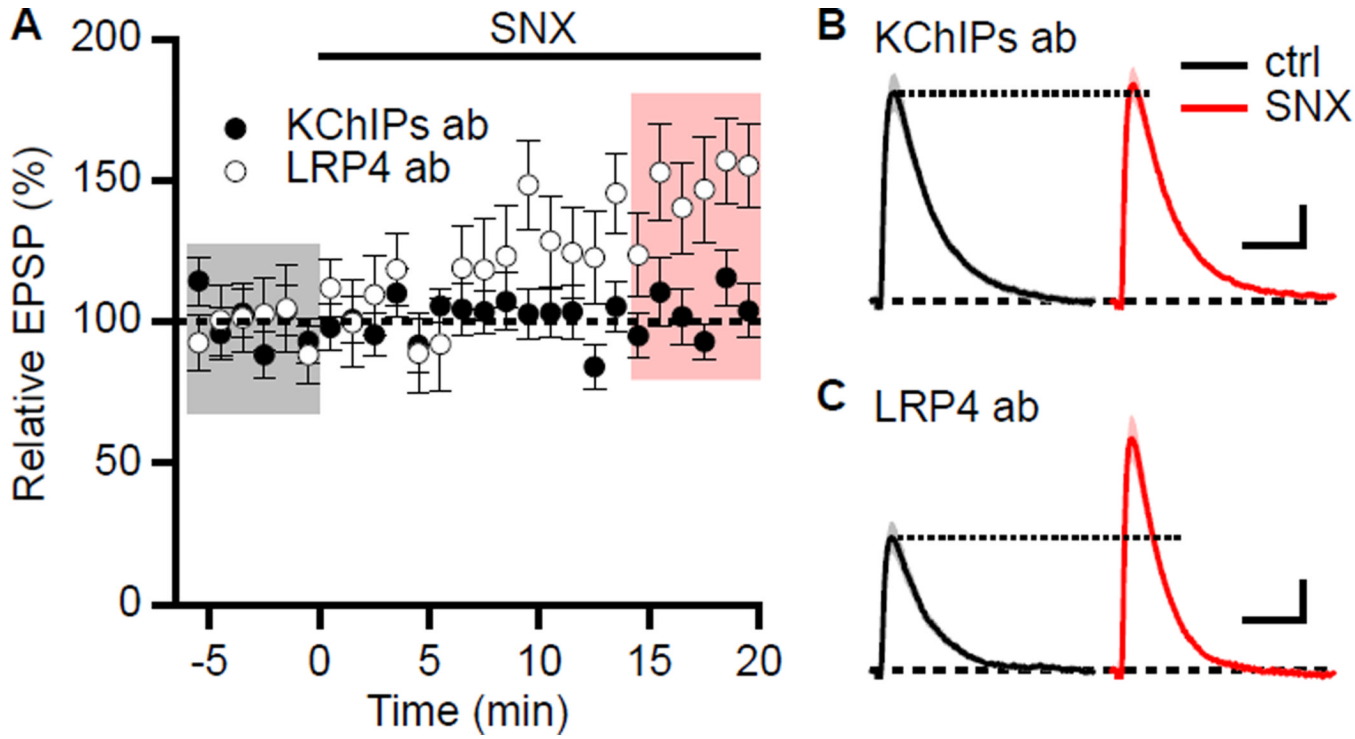

Figure 8. SNX boosting of EPSPs requires functional KChIPs

(A) Time course of normalized EPSP amplitude (mean ± s.e.m) for baseline in control aCSF and during wash-in of SNX in cells dialyzed with KChIPs antibody (closed symbols, n = 9) or LRP4 antibody (open symbols, n = 6). (B) Representative average of 18 EPSPs dialyzed with KChIPs antibody taken from indicated shaded time points in Panel A for control (baseline; black) and 14–20 min after SNX wash-in (red); shaded areas are ± s.e.m. Scale bars: 0.5 mV and 50 ms. (C) Representative average of 18 EPSPs dialyzed with LRP4 antibody taken from indicated shaded time points for control (baseline; black) and 14–20 min after SNX wash-in (red); shaded areas are ± s.e.m. Scale bars: 0.5 mV and 50 ms.